Deciphering the Mismatch Recognition Cycle in MutS and MSH2-MSH6 Using Normal-Mode Analysis

Shayantani Mukherjee,[†] Sean M. Law,[†] and Michael Feig[†‡*]
[†]Department of Biochemistry and Molecular Biology, and [‡]Department of Chemistry, Michigan State University, East Lansing, Michigan

ABSTRACT Postreplication DNA mismatch repair is essential for maintaining the integrity of genomic information in prokaryotes and eukaryotes. The first step in mismatch repair is the recognition of base-base mismatches and insertions/deletions by bacterial MutS or eukaryotic MSH2-MSH6. Crystal structures of both proteins bound to mismatch DNA reveal a similar molecular architecture but provide limited insight into the detailed molecular mechanism of long-range allostery involved in mismatch recognition and repair initiation. This study describes normal-mode calculations of MutS and MSH2-MSH6 with and without DNA. The results reveal similar protein flexibilities and suggest common dynamic and functional characteristics. A strongly correlated motion is present between the lever domain and ATPase domains, which suggests a pathway for long-range allostery from the N-terminal DNA binding domain to the C-terminal ATPase domains, as indicated by experimental studies. A detailed analysis of individual low-frequency modes of both MutS and MSH2-MSH6 shows changes in the DNA-binding domains coupled to the ATPase sites, which are interpreted in the context of experimental data to arrive at a complete molecular-level mismatch recognition cycle. Distinct conformational states are proposed for DNA scanning, mismatch recognition, repair initiation, and sliding along DNA after mismatch recognition. Hypotheses based on the results presented here form the basis for further experimental and computational studies.

INTRODUCTION

DNA mismatch repair (MMR) pathways maintain the integrity of genomic DNA by eliminating errors incorporated during replication and recombination. The initial steps of DNA-mismatch recognition and repair initiation in the postreplication MMR pathway are mostly conserved from bacteria to humans with MutS in prokaryotes and MutS homologs (MSH) in eukaryotes recognizing defective DNA and initiating repair (1–3). A functional MSH protein leading to correct mismatch recognition and subsequent deletion is especially important in humans for the avoidance of cancer phenotypes (4).

Prokaryotic MutS is comprised of monomers with identical sequence, termed S1 and S2, although it forms a structural heterodimer when bound to DNA (5,6). MutS is known to recognize base-base mismatches and short base insertions or deletions, leading to their successful repair. In eukaryotes, at least seven variants of MSH have been identified. They form a number of heterodimers, of which MSH2-MSH6 corresponds most closely to MutS (with MSH2 corresponding to S2, and MSH6 corresponding to S1) (2). Like MutS, the MSH2-MSH6 complex also recognizes basepair mismatches and single base insertions or deletions with high efficiency, but does not efficiently recognize longer base insertions or deletions (1,2).

After MutS or MSH2-MSH6 is successfully associated with a mismatch, a complex is formed in the presence of ATP with MutL in prokaryotes (7) or MutL homologs (MLH) in eukaryotes (8) to promote downstream repair events. Crystal structures of prokaryotic MutS from *Escherichia coli* (*E. coli*) (6), *Thermus aquaticus* (5), and human MSH2-MSH6 (9) bound to different basepair mismatches or a single thymine insertion/deletion have become available. The structures all show the same architecture with two main functional sites at opposite ends of the dimer: a DNA-binding site and an ATPase site. As evidenced by the crystal structures, the clamp and DNA-binding domains (domains IV and I, respectively) from both chains (S1 and S2 of MutS or human MSH2-MSH6) encircle the mismatched DNA (Fig. 1). However, only the DNA-binding domain of one of the chains is in direct contact with the mismatch, giving rise to structural and functional asymmetry between the dimer moieties. Specific contacts with the mismatch base are made through a conserved ''Phe-X-Glu'' motif in the DNA-binding domain of chain S1 in MutS and MSH6. Insertion of this motif into the minor groove of the DNA is coincident with significant DNA bending (~60°) and minor groove widening at and around the mismatch site compared to canonical DNA. The bent conformation of the DNA is further stabilized through nonspecific contacts from the clamp domain.

The nucleotide-binding domains (NBDs; domain V) reside on the opposite end of the protein with the ATP-binding sites (ATPase sites) lying close to the dimerization interface. Biochemical studies have provided evidence for functional coupling between DNA scanning, mismatch recognition, repair initiation, and ATPase activity (10–13), which suggests allosteric signaling within the MutS or MSH dimers. Each MutS ATPase domain belongs to the ATP binding casette (ABC) superfamily (14) and is comprised of functionally important residues from both

Submitted September 9, 2008, and accepted for publication October 24, 2008.

*Correspondence: feig@msu.edu

Editor: Nathan Andrew Baker.

0006-3495/09/03/1707/14 $2.00

doi: 10.1016/j.bpj.2008.10.071

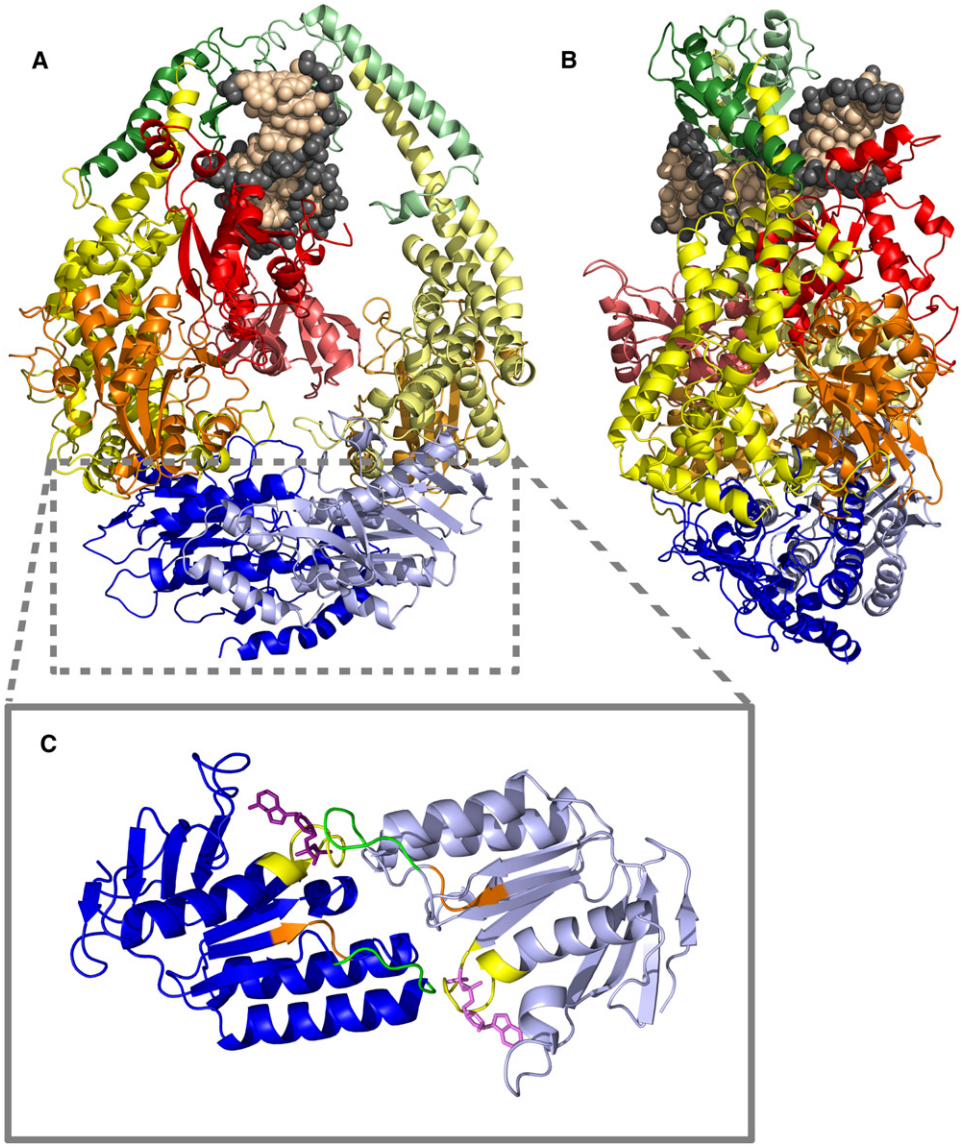

FIGURE 1 Crystal structure of MSH2-MSH6 in front (*A*) and sideways (*B*) orientation. Protein domains are indicated online in red (I, DNA binding), orange (II, connector), yellow (III, lever), green (IV, clamp) and blue (V, ATPase) and in shades of gray in print. DNA is indicated in light (base-pairs) and dark (backbone) brown, and bound ADP molecules are magenta. Darker shades refer to MSH6; lighter shades refer to MSH2. (*C*) Close-up view of the NBD highlights the Walker A motif in yellow, the Walker B motif in orange, and the signature loop in green.

chains, as shown in Fig. 1 *C* (15). The NBD residing in each particular chain consists of Walker A and Walker B loops that are important for nucleotide phosphate binding and phosphate catalysis, respectively. Another loop containing a conserved phenylalanine residue (596 in MutS, 650 in MSH2, and 1108 in MSH6) stacks with the nucleotide adenine ring and the cavity is completed by the signature loop of the opposite monomer, which has been suggested to play an important role in catalysis. Several studies have suggested that the ATPase activities of the two chains are strongly correlated with each other and follow a sequential rather than simultaneous pattern of ATP hydrolysis (10). Moreover, both sites show intrinsic asymmetry in the ATPase activity, with nucleotide-binding affinities changing significantly for each ATPase site during the recognition cycle (10–13,16). In free enzyme or when bound to regular DNA, the chain that contacts the DNA mismatch (S1 or MSH6) has a higher affinity for ATP compared to the other chain, whereas chain S2 or MSH2 binds mostly ADP (13,16). It is further known that ATP hydrolysis occurs rapidly in S1/MSH6 when the protein is bound to regular DNA and that ADP release is the rate-limiting step (11). The ATPase site of the other chain has a much slower hydrolysis rate (13). These results highlight a differential behavior of the two ATPase sites when the protein is bound to regular DNA, as depicted schematically in Fig. 2. During scanning of regular DNA, the NBD of chain S1/MSH6 binds ATP followed by fast hydrolysis to ADP. However, since exchange of ADP for ATP does not occur as rapidly as hydrolysis, ADP will be bound to this site for the majority of the time. At the same time, ADP is also bound predominantly to the other NBD of chain S2/MSH2.

Experimental data suggest that mismatch binding promotes the exchange of ADP for ATP while stalling

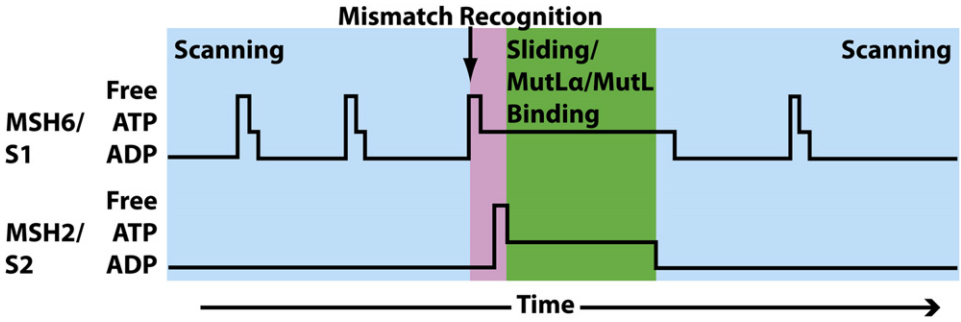

FIGURE 2 The dynamic behaviors of the ATPase site in both chains are represented along an arbitrary horizontal time axis. Alterations among three possible nucleotide-binding states (ADP/ATP/free) of the NBD are shown along the vertical axis with the help of curves that represent different hydrolysis patterns during functionally important phases of the protein.

ATP hydrolysis of S1/MSH6 (11,12). The resulting prolonged ATP-bound state at S1/MSH6 ''authorizes'' recognition of a mismatch by the DNA binding domain, whereas ATP is readily hydrolyzed when the DNA binding domain is bound to regular DNA (17). Furthermore, stable ATP binding by S1/MSH6 ultimately leads to reduced ADP-binding affinity in the ATPase site of S2/MSH2. This presumably enhances the ATP-binding affinity of S2/MSH2 (13). The dual ATP-bound state is believed to trigger a conformational change to a sliding clamp conformation whereby the mismatch is released by the DNA-binding domain and rebinding of mismatched DNA is inhibited (12,13). Of interest, a recent single-molecule study on MSH2-MSH6 demonstrated that the sliding motion along DNA after mismatch recognition is independent of ATP hydrolysis (18).

Although there is a general understanding of the long-range allostery of MutS and its homologs involved in recognition and repair initiation, the molecular-level events leading to the functional correlation between N-terminal DNA mismatch recognition and C-terminal nucleotide binding and hydrolysis have remained elusive. Further advances in this respect have been hindered by the fact that the available crystal structures show only the mismatch-bound state and do not provide information about the different nucleotide-bound combinations in the two ATPase domains. Until now, the complex interplay between functional states of the two ATPase- and DNA-binding sites has mostly been elucidated by biochemical kinetic studies that failed to provide a molecular-level understanding of the process. Experiments may continue to reveal additional information for different functional states; however, conformational sampling of proteins can also be studied by theoretical means. Molecular-dynamics simulations that often offer insights in this regard are not easily applicable to MutS because of the long timescales of the mismatch recognition process and the large system size of the MutS-DNA complex. Normal-mode analysis (NMA) is an alternative strategy for studying large-scale conformational changes in biomolecules. NMA relies on a harmonic approximation of the potential energy surface around a minimum energy structure, and the resulting lowest-frequency dynamic modes often resemble biologically relevant functional motions (19,20). Here, we applied NMA to study the conformational dynamics of MutS and its eukaryotic homolog MSH2-MSH6. The results suggest a new molecular-level understanding of the long-range allosteric pathway in the functional interplay among DNA mismatch recognition, nucleotide-binding activity, and repair initiation. A structural characterization of distinct conformational states, along with the elucidation of a complete functional cycle, offers possible avenues for validating the proposed cycle through experiments.

MATERIALS AND METHODS

Normal-mode (NM) calculations were performed on *E. coli* MutS and its human homolog, MSH2-MSH6, in the absence of any bound nucleotides. Calculations were performed on each protein in the presence or absence of DNA, resulting in a total of four sets of NM calculations. These are referred to as MSH-DNA, MSH-free, MutS-DNA, and MutS-free for MSH2-MSH6 with DNA, MSH2-MSH6 without DNA, MutS with DNA, and MutS without DNA, respectively. Initial structures of *E. coli* and human protein were obtained from Protein Database (PDB) IDs 1E3M (6) and 2O8B (9), respectively, and missing loops were constructed using MODELLER (21). The structures were then extensively energy minimized using the CHARMM22/CMAP force field (22) and distance-dependent dielectric ($\varepsilon = 4$). The root mean-square deviations (RMSDs) of the minimized structures with respect to the crystal structures were 2.08Å, 2.42Å, 1.28Å, and 2.06Å for MSH-DNA, MSH-free, MutS-DNA, and MutS-free, respectively. Low RMSD values indicate that extensive minimization in the absence of explicit water or DNA does not lead to significant structural deviations from the crystal structure. NMs were calculated by means of the block-NM approach using the VIBRAN module in CHARMM (23,24), version c33a2, and with the same force field as used for minimization. Only low-frequency modes were analyzed in both proteins because they are the most relevant for describing functional motions involving the entire complex. To calculate the similarity between individual modes among MutS and MSH2-MSH6, we defined the overlap index for each pair of modes (i,j) as $|(\sum_k S_{ik} \cdot H_{jk})/k|$, where k is the number of aligned residues of MutS and MSH, S_{ik} is the k^{th} component unit vector of the i^{th} mode of MutS, and H_{ik} is the k^{th} component unit vector of the j^{th} mode of MSH. Each dot product contributing to the sum is between unit vectors and can possess a maximum value of 1 for residue pairs moving in exactly the same direction, or a value of -1 for residue pairs moving in exactly the opposite direction. The value of the overlap index can thus reach a maximum value of 1 for an ideal case in which all aligned residues of two proteins are moving in exactly the same or opposite direction. The sequence alignment between MSH2-MSH6 and MutS was taken from previous work (9). Molecular graphics were generated using PyMOL (25).

RESULTS AND DISCUSSION

NM calculations were carried out to explore the possible conformational dynamics of MutS and MSH2-MSH6 from

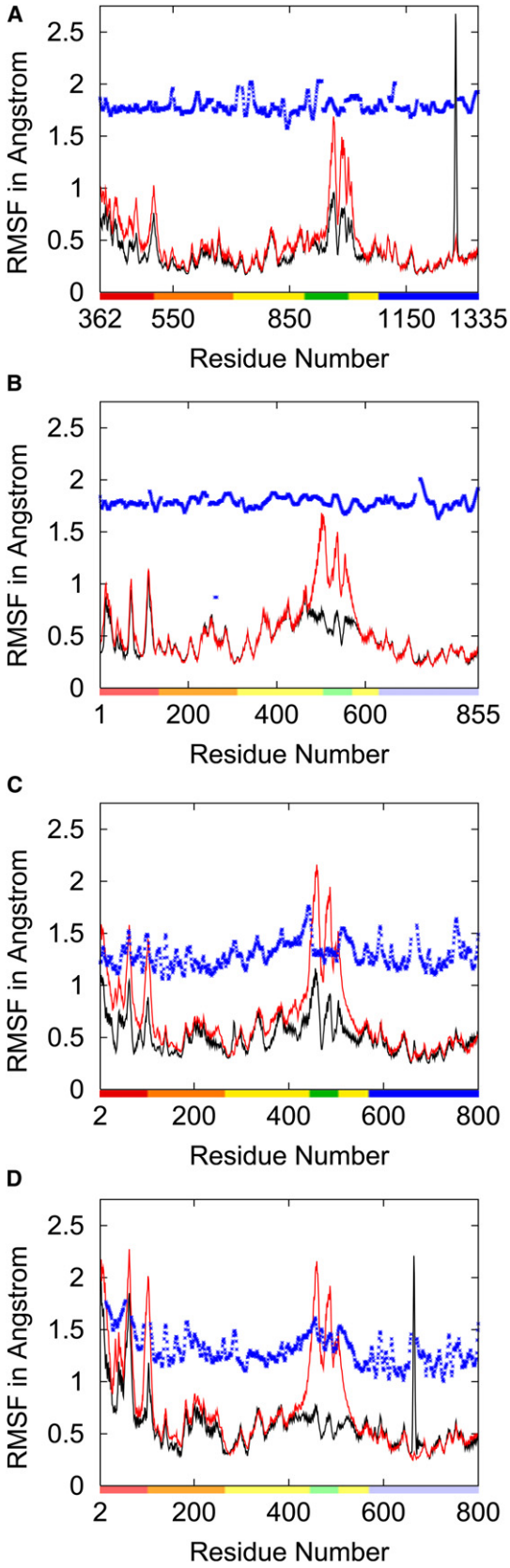

the perspective of the crystal structures. Apart from conducting NMA calculations on both proteins with bound DNA, we also considered proteins without DNA to allow dynamics beyond the DNA mismatch bound form. Results from the analysis of MutS and MSH2-MSH6 in the presence and absence of DNA are discussed below. Data from four different sets of NM calculations are referred to as MSH-DNA, MSH-free, MutS-DNA, and MutS-free for MSH2-MSH6 with DNA, MSH2-MSH6 without DNA, MutS with DNA, and MutS without DNA, respectively.

Flexibility of MutS and MSH2-MSH6 from NMs and x-ray data

Root mean-square fluctuations (RMSFs) provide information about inherent protein flexibility. They can be deduced from experimental B-factors or can be calculated from NMs (26). The results in Fig. 3, *A–D*, show that the RMSFs calculated from experimental B-factors are uniformly high due to the limited resolution of the MSH2-MSH6 crystal structure (2.75 Å) and do not provide significant information about relative domain fluctuations. RMSFs from B-factors of the MutS crystal structure (with a resolution of 2.2 Å) are still high but indicate increased flexibility in MutS domains I and IV, and parts of III, in particular for chain S2. In contrast, RMSFs calculated from the first 10 NMs show significant differences in the domain movements. MutS-free and MSH-free exhibit large flexibility in the DNA binding and clamp domains (I and IV) and a lesser degree of flexibility between the lever domains (III). In contrast, the ATPase domains (V) show comparably low structural fluctuations. Mode calculations for MutS-DNA and MSH-DNA provide qualitatively similar results, but with damped flexibility in the clamp domains and in the DNA-binding domains of chain MSH6 and MutS S1. Fig. 4, *A–D*, show both proteins colored according to the B-factors calculated from NM RMSF values.

The NMA-based dynamics of MutS and MSH2-MSH6 are remarkably similar between chains, as well as between the prokaryotic and eukaryotic enzymes. MSH6 and domain I of MSH2 appear to be slightly more rigid compared to MutS, which may relate to the functional specialization of MSH2-MSH6. One may speculate that MutS requires increased flexibility to recognize both mismatches and longer insertions/deletions, in contrast to MSH2/MSH6, which recognizes only mismatches and single base insertions/deletions. Although an absolute comparison of RMSF

FIGURE 3 RMSF of Cα atoms as a function of residue number calculated from the first 10 NMs (online: *red*, without DNA; *black*, with DNA) and from crystallographic B-factors according to $\mathrm{RMSF}_{\mathrm{Xray}} = \sqrt{3B/8\pi^2}$ (*blue*, *thick dots*) for MSH6 (*A*), MSH2 (*B*), MutS S1 (*C*), and MutS S2 (*D*). Discontinuities in the RMSF x-ray curve are due to missing residues in the crystal structures. Protein domains are indicated by colored bars (online), with red, orange, yellow, green, and blue for domains I, II, III, IV, and V, respectively. Chain MSH6/MutS S1 is indicated by dark shades, and MSH2/MutS S2 is indicated by light shades.

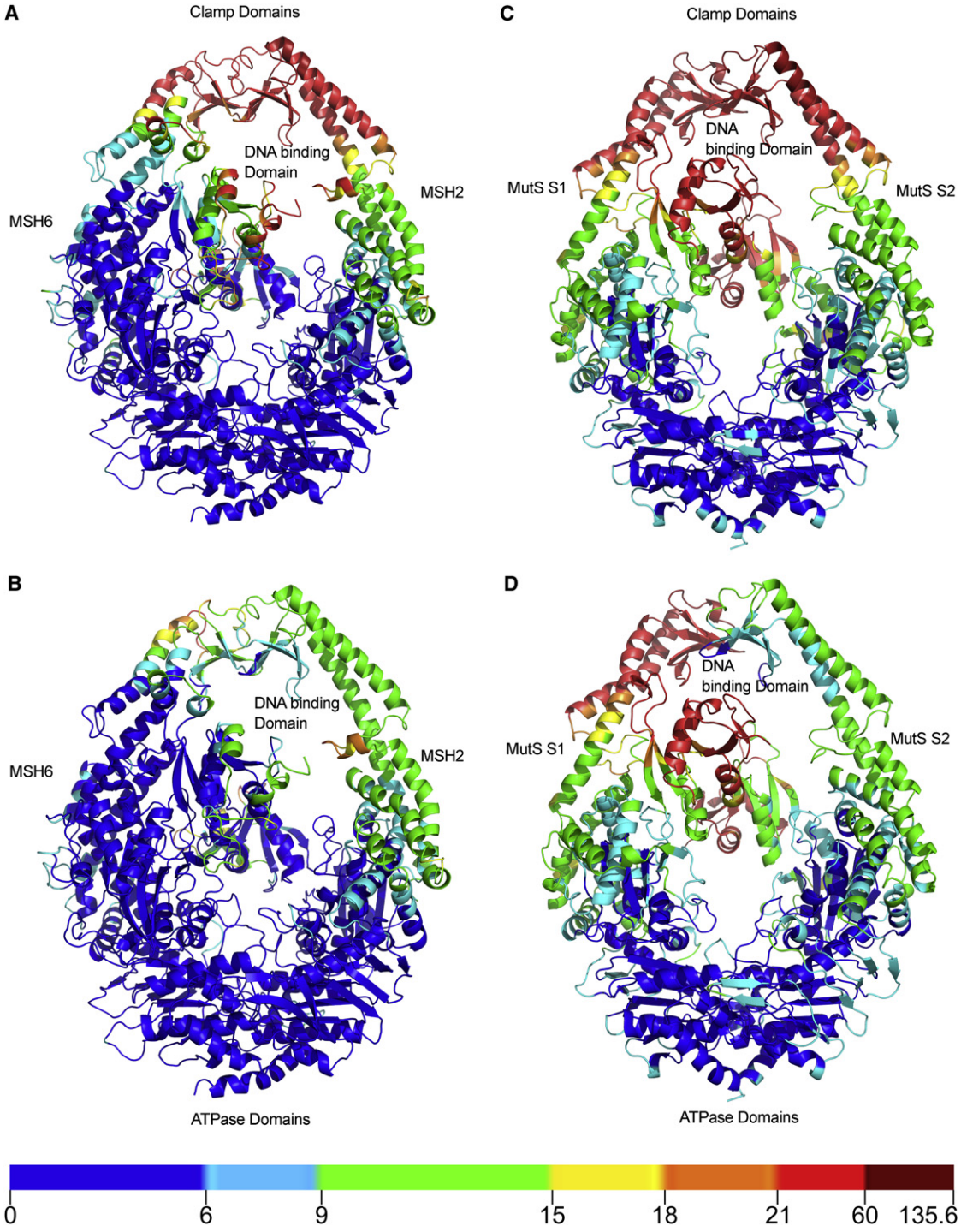

FIGURE 4 Protein backbone showing thermal fluctuations color-coded by B-factors calculated from RMSF of the first 10 modes for MSH-free (*A*), MSH-DNA (*B*), MutS-free (*C*), and MutS-DNA (*D*). The color scale for B-factors is provided at the end of the figure.

values from a small number of NMs between proteins of different sizes may be problematic, very similar results were obtained when motions of the first 100 modes were accumulated (data not shown).

Furthermore, it appears that MSH2 and MutS S2 are slightly more flexible than MSH6 and MutS S1, respectively, with the exception of the clamp domain for MSH-DNA and MutS-DNA systems. The increased flexibility in domain I of MSH2 or MutS S2 and the decreased flexibility of the clamp domain compared to the other chain correspond to the structural asymmetry of MutS and MSH2-MSH6. The increased flexibility of domain I of MSH2/MutS S2 probably results from the fact that they do not make considerable contacts with the DNA, whereas extensive DNA contacts of the

clamp domains of MSH2/MutS S2 compared to the other chain accounts for its decreased flexibility. It was observed that the clamp domain of MSH2 and MutS S2 makes 83 and 86 atomic contacts with the DNA, respectively, whereas that of MSH6 and MutS S1 makes only 62 and 42 contacts, respectively. It was further observed that the clamp and lever domains of MutS S1 are more flexible compared to those of MSH6, which again is a result of fewer atomic contacts made by the clamp of S1 with the DNA compared to MSH6. The number of atomic contacts was calculated by considering protein heavy atoms around 5Å of the DNA in the minimized structure of both proteins. Finally, Fig. 4 highlights that the clamp and lever domains of MSH2 in MSH-DNA are slightly more flexible than the corresponding domains in MutS S2 of MutS-DNA. These differences are probably the result of the proteins being bound to DNA segments of varying lengths. MutS-DNA has a longer DNA (3 basepair steps more than MSH-DNA), which topologically constrains the mobility of MutS S2, giving rise to a more rigid S2 clamp compared to that of MSH2. The portion of the lever domain of S2 that is tightly connected to the clamp also undergoes some degree of rigidification. The rigidification of MutS S2 may be more close to reality, as DNA undergoing repair in the cell is much longer than that observed in the crystal structures. It should also be mentioned that substantially longer DNA can alter the extent of flexibility observed in the clamp of the other chain, namely, S1 and MSH6. Hence, difference in the flexibility of clamp and lever due to the presence of a much larger DNA cannot be directly inferred from these studies using fragmented DNA. The only observed fact is that an overall decreased flexibility of the clamps and levers will result in both chains when compared to DNA-free systems.

Finally, it was observed that the RMSF for protein with DNA spikes at residues 1275–1281 in MSH6 and residues 663–666 in MutS S2. This is likely a manifestation of the tip effect (27) and is considered physically meaningless.

Correlated motions in MutS and MSH2-MSH6

Covariance plots averaged over the 10 lowest NMA modes were calculated to examine correlated motions in all four systems under investigation. The results shown in Fig. 5 indicate similar overall correlations in MutS and MSH2-MSH6 in the absence and presence of DNA. Furthermore, both chains of MutS and MSH2-MSH6 show similar average correlation patterns, with only minor variations, despite the structural asymmetry of the complex. Common to all chains are correlations within each domain, reflecting rigid-body domain motions, such as correlations between adjacent domains II (connector domain) and III (lever domain), between III and V (ATPase domain), and between I (DNA binding domain) and II. Whereas correlations within the same subunit are generally positive, correlations between dimer moieties are mostly negative, with the exception of a strong positive correlation between the two ATPase domains and the two clamp domains as a result of dimerization.

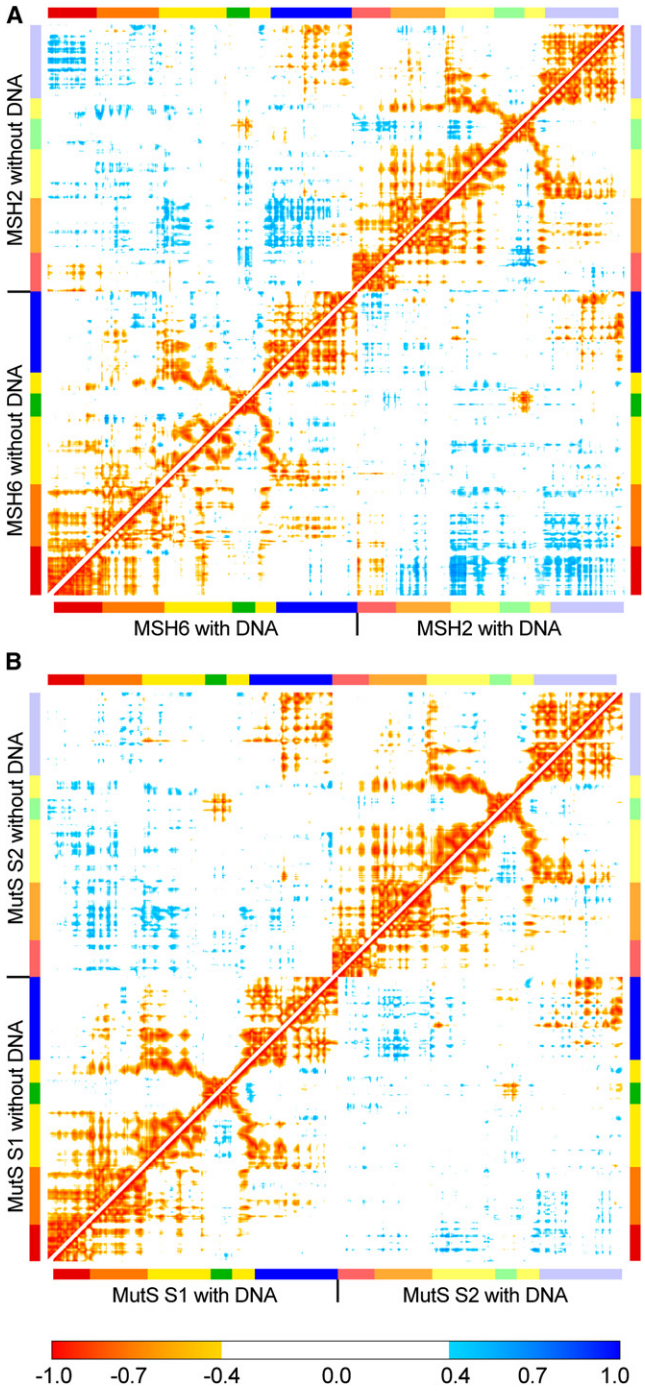

FIGURE 5 Average covariance from the first 10 modes in MSH2-MSH6 (*A*, *upper triangle*: MSH-free; *lower triangle*: MSH-DNA) and MutS (*B*, *upper triangle*: MutS-free; *lower triangle*: MutS-DNA). Protein domains in both chains are indicated by colored bars following the same color scheme as in Fig. 3.

The plots indicate a high positive correlation between the lever domains and parts of the ATPase domains immediately

adjacent to the lever, including the ATPase-binding sites. Experiments suggest the presence of long-range allostery between the N-terminal DNA-binding domain and the C-terminal ATPase domains; however, a clear understanding of the allosteric pathway is lacking. Strong correlations between the ATPase sites and lever domains highlight the propagation of signals within the two functional sites via the levers. Furthermore, the DNA-binding domain in MSH6 and MutS S1 has a strong negative correlation with the ATPase domain in MSH2 and MutS S2, respectively, in particular for MSH-DNA and MutS-DNA, again suggesting conserved domain motions that are important for allostery.

Correspondence between MutS and MSH2-MSH6 modes

The analysis of RMSFs and motional correlations indicates that MutS and MSH2-MSH6 exhibit similar dynamic characteristics in both the presence and absence of DNA. Furthermore, the correlation analyses from the first 10 modes suggests dynamic coupling between DNA binding and ATPase activity. To explore this point in more detail, the 10 lowest-frequency modes were individually compared between different states of the same protein, i.e., between MSH-free and MSH-DNA or between MutS-free and MutS-DNA. The same comparison was also performed between different proteins, i.e., MSH-free and MutS-free and MSH-DNA and MutS-DNA. Table 1 shows the overlap indices calculated between any pair of modes from four different systems as described in Materials and Methods. An overlap index value of 1.0 means that atoms move in identical directions in the two modes that are compared, and a value of 0.0 means that motions are entirely orthogonal or that atom motions have zero amplitude. Although a value of 1.0 or close to it is unlikely even for very similar structures, visual inspection of the MutS and MSH modes indicates that the motions are qualitatively similar when overlap indices are at 0.6 and above and, to a lesser but still substantial extent, when values are between 0.5 and 0.6, especially when MutS is compared with MSH. Relatively low overlap indices despite visually similar motions are due to uncertainties in the alignment between the two proteins, with a sequence identity of only 21% and 24% for MSH2 and MSH6 (9); differences in structure; and significant overall flexibility due to the multidomain nature of both MutS and MSH.

Table 1 shows that the highest degree of overlap on a mode-by-mode basis exists between MSH-free and MSH-DNA, and also between MSH-free and MutS-free systems. There is a lesser degree of one-to-one correspondence between MutS-free and MutS-DNA, and also between MSH-DNA and MutS-DNA, with individual modes being reordered more significantly according to frequencies in these systems. High one-to-one overlap is found between modes 1, 2, 3, 4 of MSH-free and modes 1, 5, 3, 4 of MutS-free; between modes 1, 3, 4, 9, 10 of MSH-DNA and modes 2, 5, 4, 9, 10 of MutS-DNA; between modes 1, 2, 4, 5, 8, 9 of MSH-DNA and modes 2, 3, 4, 5 and 9, 10, 7 of MSH-free; and between modes 1, 2, 3, 5 of MutS-DNA and modes 2, 5, 3 and 9, 7 of MutS-free. It is apparent that many modes do not match on a one-to-one basis, but share common features with multiple modes (e.g., mode 2 of MSH-free matches modes 2, 5, and 8 of MutS-free). It is known from previous studies that the complex domain motions that are responsible for altered functional states in a large protein are often better represented as a combination of low-frequency modes. Our studies also suggest that the low-frequency modes of both MSH and MutS exhibit almost similar domain flexibility, whereas specific protein dynamics are often seen to occur as a combination of multiple modes showing different degrees of mode mixing in both proteins. The degree of mode mixing observed in this study will likely change as a result of using different force fields or coarse-grained models, but low-frequency NM space will likely be conserved in all NM analyses, provided the starting structure remains the same. Thus, the main aim of this study is to highlight the conserved nature of domain motions in both proteins, rather than to highlight any specific mode or modes responsible for the protein function.

The presence of DNA alters the structural flexibility to some extent, as evidenced by the differences between modes in the presence and absence of DNA. For example, mode 1 is present in MSH-free and MutS-free but not in MSH-DNA or MutS-DNA. As described in more detail below, the mode involves large motions of the clamp domains that are not possible in the presence of DNA. Visual inspection further reveals that altered motions of the clamp and DNA-binding domains for structures in the presence and absence of DNA is a major factor in reduced mode overlap indices between the two protein systems, despite otherwise similar overall motion. Of interest, MSH modes are much more conserved in MSH-free and MSH-DNA systems than in the two MutS systems. This suggests that protein flexibility is altered more in MutS than in MSH2-MSH6 through specific DNA interactions, especially near the DNA-binding domain and clamps. This further reflects a more rigid overall structure in MSH2-MSH6 that is optimized to interact with mismatched DNA, whereas MutS requires more structural flexibility to interact with both mismatched DNA and significantly distorted DNA structures with insertions or deletions.

In this study, we focus more on modes from MSH-free and MutS-free because they are more likely to indicate motions from the known mismatch-bound crystallographic structures toward alternate states during DNA scanning and MMR. A comparison of the modes between MSH-free and MutS-free indicates that modes 1, 3, 4, and 9 from both complexes significantly overlap and may be

TABLE 1 Overlap index for a pair of modes, each from two different sets

Mode No.	1	2	3	4	5	6	7	8	9	10
MSH-free (rows) versus MutS-free (columns)										
1	***0.8***	0.1	0.2	0.2	0.0	0.1	0.2	0.3	0.2	0.1
2	0.2	**0.5**	0.1	0.0	***0.6***	0.1	0.3	**0.5**	0.0	0.1
3	0.0	0.3	***0.8***	0.3	0.2	0.2	0.1	0.0	0.3	0.1
4	0.2	0.1	0.2	***0.6***	0.3	**0.5**	0.3	0.3	0.2	0.1
5	0.1	**0.5**	0.1	0.1	**0.5**	0.4	0.3	0.2	0.1	0.2
6	0.1	0.0	0.1	**0.5**	0.2	0.3	0.3	0.3	0.4	0.1
7	0.2	0.2	0.1	0.1	0.3	0.0	**0.5**	0.3	0.3	**0.5**
8	0.3	0.2	0.1	0.1	0.0	0.4	**0.5**	**0.5**	**0.5**	0.0
9	0.1	0.2	0.2	0.2	0.2	0.4	0.1	0.0	***0.6***	0.3
10	0.1	0.3	0.1	0.3	0.0	0.4	0.2	0.1	0.2	0.3
MSH-DNA (rows) versus MutS-DNA (columns)										
1	**0.5**	***0.6***	0.4	0.0	0.0	0.0	0.0	0.2	0.0	0.1
2	0.3	**0.5**	0.4	0.1	0.1	0.2	0.1	0.3	0.1	0.2
3	0.3	0.2	0.2	0.2	***0.8***	0.0	0.4	0.0	0.2	0.0
4	0.3	0.2	**0.5**	***0.6***	0.2	0.3	0.0	0.1	0.2	0.0
5	0.0	0.1	0.2	0.3	0.2	**0.5**	0.3	0.1	0.3	0.1
6	0.3	0.2	0.0	0.2	0.3	**0.5**	0.0	0.1	0.2	0.4
7	0.3	0.0	0.1	0.4	0.0	0.4	0.0	0.3	0.1	0.2
8	0.1	0.1	0.1	0.1	0.1	0.2	0.1	0.0	0.2	0.4
9	0.1	0.2	0.0	0.2	0.2	0.0	0.1	0.0	***0.7***	0.1
10	0.1	0.0	0.2	0.1	0.1	0.2	0.4	0.4	0.1	***0.6***
MSH-DNA (rows) versus MSH-free (columns)										
1	**0.5**	***0.7***	0.0	0.1	0.3	0.0	0.2	0.1	0.0	0.2
2	0.1	0.0	***0.9***	0.1	0.2	0.0	0.2	0.2	0.1	0.2
3	**0.5**	0.4	0.1	0.2	0.4	0.4	0.3	0.4	0.2	0.2
4	0.2	0.1	0.1	***0.9***	0.2	0.3	0.2	0.3	0.3	0.0
5	0.2	0.0	0.2	0.0	***0.6***	0.2	0.4	0.1	***0.7***	0.0
6	0.2	0.2	0.2	0.1	0.0	0.4	0.3	0.0	0.2	0.2
7	0.0	0.0	0.2	0.0	0.1	**0.5**	0.2	0.2	0.4	0.1
8	0.0	0.2	0.0	0.1	0.3	0.3	0.1	0.1	0.0	***0.8***
9	0.0	0.1	0.3	0.1	0.1	0.2	***0.7***	0.2	0.2	0.0
10	0.0	0.0	0.1	0.0	0.2	0.4	0.2	0.4	0.1	0.1
MutS-DNA (rows) versus MutS-free (columns)										
1	**0.5**	***0.6***	0.4	0.3	0.2	0.3	0.3	0.4	0.1	0.0
2	0.4	0.3	0.2	0.3	***0.6***	0.1	0.2	0.4	0.1	0.2
3	0.2	0.2	***0.7***	0.3	0.1	0.2	0.1	0.1	***0.6***	0.1
4	0.1	0.2	0.4	0.2	0.0	**0.5**	0.3	**0.5**	0.3	0.4
5	0.2	0.2	0.0	0.3	**0.5**	0.4	***0.6***	0.0	0.1	0.1
6	0.3	0.1	0.2	**0.5**	0.1	0.1	0.2	0.3	0.0	0.2
7	0.4	0.3	0.1	0.0	0.4	0.0	0.2	0.1	0.4	0.3
8	0.1	0.1	0.2	0.1	0.3	0.2	0.3	0.3	0.2	0.2
9	0.2	0.1	0.2	0.2	0.2	0.2	0.2	0.4	0.1	0.3
10	0.2	0.2	0.2	0.1	0.1	0.2	0.0	0.1	0.3	0.3

Values ≥ 0.5 are in bold; values ≥ 0.6 are also in italic.

considered equivalent. Modes 2 and 5 overlap significantly, suggesting that these modes are simply reordered with respect to their frequencies. However, there is also overlap between mode 2 of both complexes, suggesting common features in both modes. Otherwise, there is significant mode overlap along the diagonal for modes 7–9 and additional limited off-diagonal overlap for modes 6–10. Overall, mode overlaps between MSH-DNA and MutS-DNA are lower, but high overlap indices are again limited mostly to diagonal or nearby off-diagonal elements, with modes 1, 2, 3, 4, 5, 6, 9, and 10 of MSH-DNA corresponding to modes 1 and 2, 2, 5, 4, 6, 6, 9, and 10 of MutS-DNA.

Low-frequency modes in MSH2/MSH6

Our analyses indicate that the dynamic characteristics are largely conserved between MutS and MSH2-MSH6 in both the presence and absence of DNA. This is not surprising, but it is also not trivial given the structural differences between the eukaryotic and prokaryotic enzymes and the slightly different biological functions. In the following, we describe the lowest-frequency modes in more detail, with a focus on the modes of MSH-free.

The protein motion during each of the first five modes of MSH-free is shown in Fig. 6. Close-up views of the ATPase domains of selected modes are shown in Fig. 7. Modes 6–10

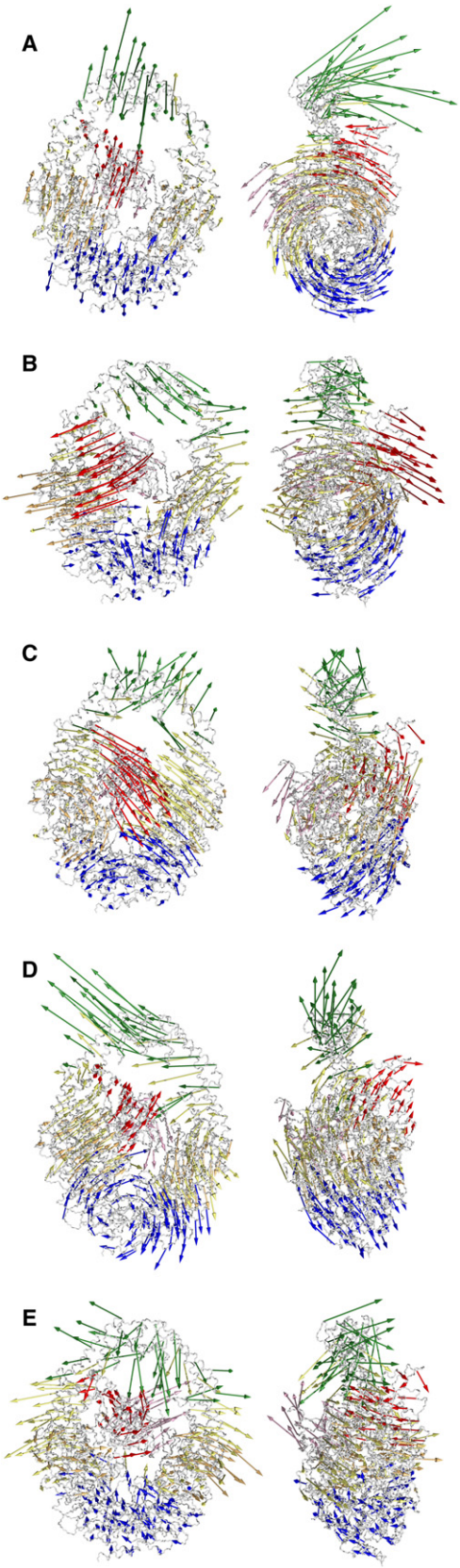

of MSH-free and all 10 modes of MutS-free and MutS-DNA, as well as those for MSH-DNA, are shown in Figs. S1–S5 in the Supporting Material. Movies for mode 1 (Movies S1a and S1b), mode 2 (Movies S2a and S2b), mode 3 (Movies S3a and S3b), mode 4 (Movies S4a and S4b), and mode 5 (Movies S5a and S5b) of MSH-free are also provided. Initial visual inspection suggests the following general conclusions about the nature of domain motions in both MutS and MSH2-MSH6: 1), Most of the modes show an overall breathing motion of the DNA-binding cavity involving the clamp and DNA-binding domains. The parts of the clamp domains that are directly bound to the DNA backbone always show damped motion in proteins with DNA, although movements of other parts of the DNA-binding cavity show a similar kind of breathing motion. Such an opening/closing motion of the DNA-binding cavity corresponds to conformational transitions between a mismatch-bound state and scanning/sliding conformations where the interaction with DNA is presumed to be weaker. 2), Many modes show a correlation between opening/closing of the DNA-binding cavity and alterations in the ATPase domain, in particular the nucleotide-binding cleft. This finding establishes that both MutS and MSH2-MSH6 are capable of allosteric communication between DNA-binding and ATPase activity. The correlation between motions of the DNA-binding domains and the ATPase domains varies because it may involve the MSH6, MSH2, or both ATPase domains in an alternating fashion. 3), A mode that affects the nucleotide-binding cleft in both ATPase domains in the same manner and at the same time is not observed in any of the four cases studied. This finding agrees with the experimental evidence that ATPase activity in MSH2-MSH6 involves the two domains in a sequential rather than a simultaneous fashion (10).

The individual modes are described in detail below:

Mode 1 involves a wagging motion of the clamp domain along the direction of the DNA. The rotating motion around the core, which is apparent in the rest of the enzyme, results from a fixed center of mass. If the protein is aligned at domains I, II, III, and V, only the clamp domain IV moves in this mode. Mode 1 involves both chains to the same extent. The exact functional role of this mode is unclear, but it may be related to the translocation of MSH2-MSH6 along DNA in the absence of mismatch when the clamps do not establish strong contacts with the DNA backbone. This mode is absent in both proteins bound to DNA mismatch, presumably due to residue contacts with the bent DNA.

Mode 2 consists of a partial opening/closing motion of the DNA-binding site that is less pronounced than in some of the other modes. The unique aspect of this mode is the

FIGURE 6 Mode motions of MSH-free projected onto the minimized crystal structure for modes 1 (*A*), 2 (*B*), 3 (*C*), 4 (*D*), and 5 (*E*). Motions are indicated by colored arrows (online) in the direction of the mode vectors for every sixth residue. Motions involving the clamp, DNA-binding, and ATPase domains are shown in green, red, and blue, respectively.

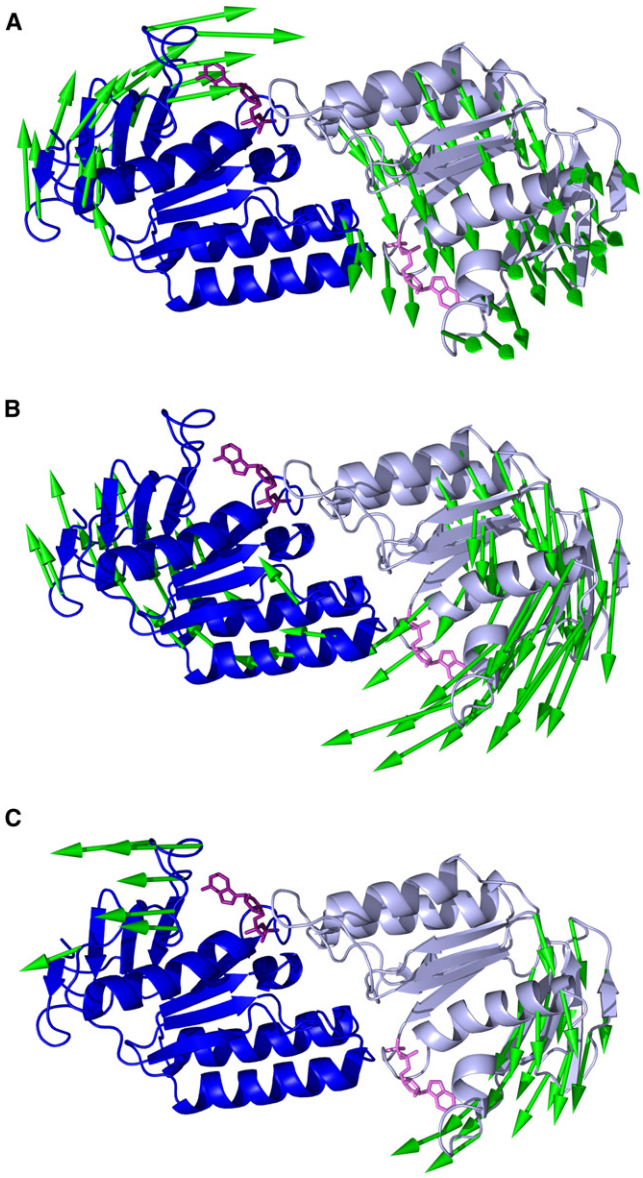

FIGURE 7 Close-up views of the motions in the NBD of MSH-free during modes 2 (*A*), 3 (*B*), and 5 (*C*). Arrows are placed on each Cα atom in every three consecutive residues, and only displacements of more than 1Å are shown. The two chains and bound nucleotides follow the same color scheme (online) as in Fig. 1 *C*.

alternating opening/closing of the nucleotide-binding clefts between the MSH2 and MSH6 ATPase domains (Fig. 7). It appears likely that this mode is involved in coupling MSH6 and MSH2 ATPase activity in a sequential fashion. As mentioned above, mode 2 in MSH-free has high overlap with mode 5 of MutS-free. However, this is due to similar motions in the DNA-binding, clamp, and core domains. The alternating opening/closing of the two nucleotide-binding sites is not present in mode 5 of MutS-free, but is seen instead in mode 2 of MutS-free. An alternating ATPase movement that correlates similarly to motions in the DNA-binding cavity is also observed in mode 1 of MutS-DNA and MSH-DNA, suggesting that the interdomain correlation is conserved in all systems.

Mode 3 couples opening of the DNA-binding site with closing of the nucleotide-binding cleft in MSH2. The opening of the DNA-binding site is achieved by the movement of the clamp domains away from the DNA, as well as the movement of the DNA-binding domain in MSH6 out of the plane of the MSH2-MSH6 complex. Relative to the DNA, this motion moves domain I out of the DNA groove rather than along its helical axis. In the open form of this mode, most DNA contacts of MSH6 near the mismatch site are lost and the DNA can essentially slide freely relative to MSH2-MSH6. This mode is highly conserved in all other systems of MutS and MSH, and is thus expected to play an important role in the protein's functional cycle. An almost identical mode is observed for modes 2 and 3 for MSH-DNA and MutS-DNA. We note, though, that the overlap index between the two modes in MSH-DNA and MutS-DNA is small due to altered clamp movements in MutS-DNA, but otherwise they show similar domain motions.

Mode 4 consists mainly of a sideways motion of the clamp and part of the lever domains toward either the MSH2 or MSH6 side of the enzyme. This mode is asymmetric with respect to the overall complex. A symmetric version of this mode would result in clamp domain separation and lead to an open dimer where the clamp domains are far away from each other, as proposed for the DNA-free complex from small-angle x-ray scattering (28). The symmetric mode is not observed, presumably due to limitations of the harmonic approximation in NMA.

Mode 5 involves closing of the DNA-binding cavity that is coupled with opening of the nucleotide-binding cleft in MSH6. The closing of the DNA-binding cavity is achieved primarily by the motion of the clamp domains directly toward the DNA. A similar overall motion is also found in mode 2 of MutS-free, although the coupling between opening and closing of the DNA-binding cavity with changes in the ATPase domain of MutS S1 is more pronounced in mode 6 of MutS-free. It is likely that MutS-free achieves a motion equivalent to the MSH-free mode 5 through a combination of modes 2 and 6. A similar correlated motion between the DNA-binding cavity and ATPase domains is further observed in mode 5 of MSH-DNA and mode 4 of MutS-DNA.

Functional cycle of MSH2-MSH6 and MutS from NMs

The crystal structures of MutS and the MSH2-MSH6 complex show only the mismatch-bound conformation. It is clear, however, that other functional states are involved during scanning of regular DNA, authorization of MMR, and sliding of the enzyme along DNA during and immediately after repair before DNA scanning is resumed. On the

molecular level, these different states are likely reflected in altered conformations of MSH2-MSH6 and MutS. X-ray crystallographic approaches have not identified alternate states of MSH2-MSH6, but there is evidence of alternating ATP- and ADP-bound states from small-angle x-ray scattering (28), where ATP binding has resulted in more compact protein conformations. The NMA presented here offers for the first time, to our knowledge, insights into the functional dynamics of MSH2-MSH6 and MutS beyond the known DNA-mismatch bound crystal structures. By combining the conserved low-frequency modes in a sequential fashion, it is possible to propose, for the first time, a complete functional cycle of MSH2-MSH6 and MutS that is in full agreement with experimental observations. The proposed molecular-level picture of the cycle is illustrated in Fig. 8 and described in detail below.

DNA binding

The functional cycle of MSH2-MSH6 and MutS begins with binding to newly replicated DNA. Experimental data suggest that DNA-free MutS is present in an open form. Upon association with DNA, the clamp domains are presumed to close. The asymmetric mode 4 indicates how the clamp domains might separate, starting from the DNA-bound form, without significantly affecting the structure of the rest of the enzyme.

DNA scanning and mismatch recognition

Once MSH2-MSH6 or MutS is bound to DNA, it will begin scanning for base mismatches. According to single-molecule experiments, MSH2-MSH6 moves along regular DNA via one-dimensional diffusion (18), whereas DNA-binding kinetics indicate that the protein is not bound strongly to DNA in the absence of a mismatch (1,29,30). In contrast, MSH2-MSH6 and MutS interact closely with mismatched DNA in a highly bent form, as evidenced by the crystal structures (5,6,9). The formation of highly bent DNA is greatly facilitated by the presence of base mismatches or base insertions/deletions (31) and is believed to be the main feature by which mismatch DNA basepairing is recognized (1). The transition from scanning to mismatch recognition is therefore expected to involve a significant change in the DNA-binding domain from a relaxed conformation with relatively weak protein-DNA interactions to a tightened conformation in which the enzyme holds on to highly bent DNA. The

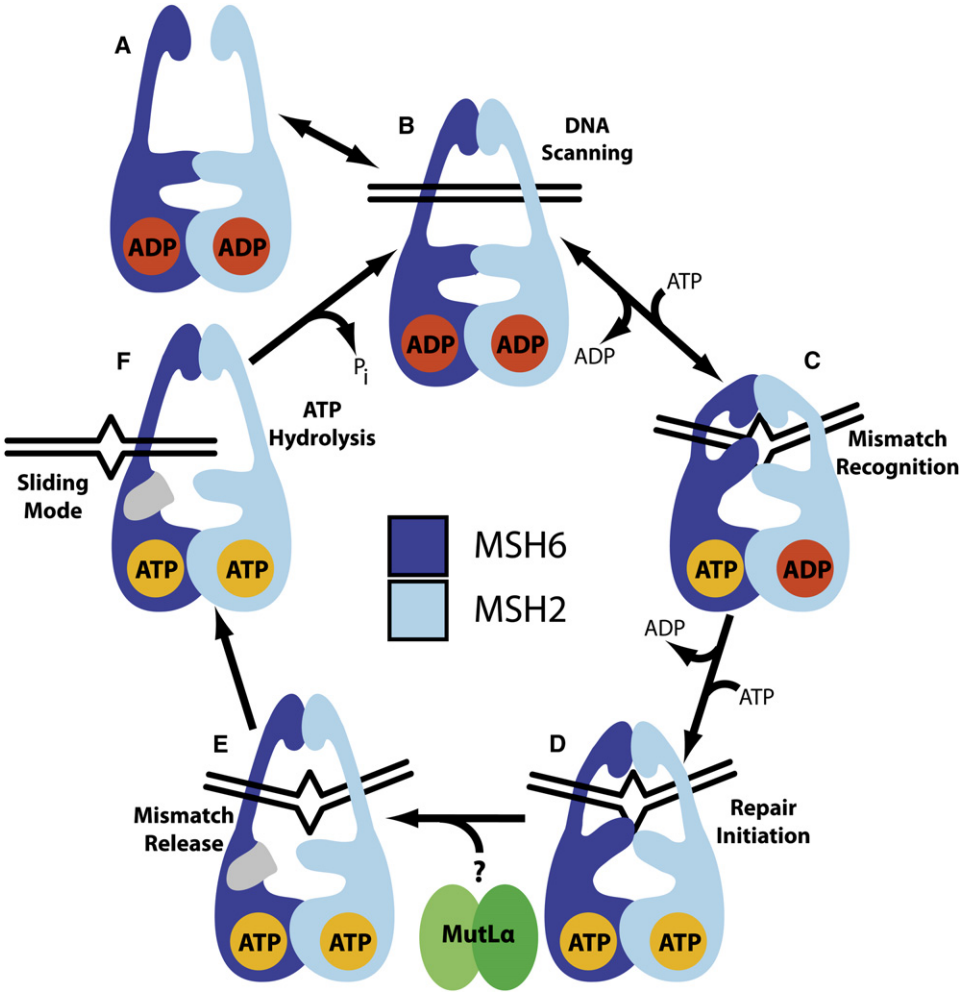

FIGURE 8 Schematic diagram representing distinct conformational states during the functional cycle of MSH2-MSH6 or MutS.

opening/closing motion of the DNA-binding cavity in mode 5 of MSH2-MSH6 describes such a transition in molecular detail.

The transition from DNA scanning to mismatch recognition is coupled to the fast exchange of ADP to ATP and subsequent stalling of ATP hydrolysis in MSH6, according to kinetic experiments (10–13). Mode 5 couples closing of the DNA-binding cavity to opening of the MSH6 or MutS S1 nucleotide-binding cleft, and vice versa. The nucleotide-binding cleft is sandwiched between the Walker A motif and a loop, which acts as a flap over the adenine moiety. This loop contains a conserved Phe residue (Phe^{596} in MutS, Phe^{650} in MSH2, and Phe^{1108} in MSH6) that stacks with the adenine ring in all available crystal structures. Previous studies of ATP binding in some ATPases revealed that binding often induces tightening of the site that is required for ATP hydrolysis, as suggested by an increase in the hydrophobicity of the binding pocket (32) or closing of specific loops in the presence of the nucleotide, resulting in a tightened cavity (33). We hypothesize that an open nucleotide-binding cleft in the MSH2-MSH6 and MutS ATPase domains encourages ATP binding but inhibits hydrolysis. In contrast, closing of the ATPase cavity predominantly involves movement of the loop bound to the adenine ring toward the catalytic center (Walker B motif), thereby ensuring successful ATP catalysis. Mode 5 therefore provides a molecular-level picture of how mismatch recognition through deformation of DNA at the mismatch site might be coupled to the experimentally observed changes in MSH6 ATP activity.

In most of the crystal structures of MSH2-MSH6 and MutS, ADP or a nonhydrolyzable ATP analog is present in both or any one of the chains, although only one MutS structure with bound ATP on both chains has been reported so far (15). The difficulties of observing the protein with stable ATP bound MSH6/S1 may be attributed to crystal packing that does not allow the formation of ATPase domains that are truly catalytically inactive (15). Thus, the crystal structure with ATP at S1 may not be fully representative of the true nonhydrolyzable state of the protein; rather, it may represent a different trapped intermediate state.

Initiation of repair

The next step after base mismatch recognition is initiation of the repair process. This involves binding of MutL/MLH to MutS/MSH2-MSH6 (1–3), which then signals further downstream events. Furthermore, kinetic studies indicate that ADP exchanges for ATP in the MSH2 ATPase domain subsequent to ATP binding in the MSH6 ATPase domain (13). The sequential coupling of ATP binding to the two ATPase domains mirrors alternating ATP hydrolysis activity in other dimerized ATPase domains as in ABC transporters (34), and can be understood in terms of the alternating opening/closing of the nucleotide-binding clefts seen in mode 2. We hypothesize that the initially very open ATP-binding site in MSH6 after mismatch recognition partially closes upon ATP binding, which in turn leads to opening of the MSH2 ATP-binding site according to mode 2 and subsequent exchange of ADP for ATP in MSH2. Mode 2 also involves structural rearrangement outside the ATPase domain, indicating that the enzyme assumes a distinct conformation at this step of the functional cycle, possibly to facilitate MutL/MLH binding.

Repair and mismatch release

Recent experiments suggest that after the initiation of repair, MSH2-MSH6 and MutS form a mobile clamp state that slides along the DNA in search of downstream repair proteins (12,13,18,35,36). A transition from the mismatch-bound state to a sliding conformation requires reopening of the DNA-binding cavity to a form that still holds the DNA but is not competent to rebind mismatched DNA (12). Moreover, this sliding activity is not powered by ATP hydrolysis. This transition remains to be elucidated by experimental studies. We propose that the most conserved mode in both proteins, i.e., mode 3, describes the molecular events involved in the formation of sliding clamp conformation. In mode 3, the DNA-binding cavity is opened by the release of the clamps from the DNA coupled to a large motion of the DNA-binding domain perpendicular to the DNA helix. As a result, intimate interactions with the mismatch through the DNA groove become impossible. This is particularly true for interactions involving the highly conserved Phe-X-Glu motif, which is known to interact specifically at the mismatch site (5,6,9,15). The protein is capable of sliding along the DNA in this state. The release of DNA mismatch binding and sliding according to mode 3 is coupled to a tightening of the MSH2 ATP-binding site, which would facilitate eventual ATP hydrolysis in MSH2 and allow recovery of the DNA scanning mode.

Although specific NMs have been mentioned in descriptions of molecular events during scanning, mismatch binding, and sliding clamp formation, it is likely that opening and closing of the DNA-binding cavity actually occurs as a result of multiple low-frequency modes. This is even more likely because almost all of the low-frequency modes studied, except mode 1 in MSH-free and MutS-free, exhibit some kind of breathing motion of the DNA-binding cavity that involves different domain motions, such as those of the clamps, levers, and DNA-binding domain. The specific modes used to describe the conformational changes in the functional cycle only show the necessary synchronization between the opening/closing of the DNA-binding cavity and the ATPase cleft, and thus are used to describe the experimentally observed allosteric effects.

Validation through experiments and further simulation

The results from the NM calculations presented here allow us to make a number of predictions about the functional

dynamics of MutS and MSH2-MSH6 and the existence of additional functional states that have not been characterized on a molecular level to date. In particular, we propose molecular-level details of long-range allosteric coupling between the N-terminal DNA-binding domains and the C-terminal ATPase sites, as well as coupling between the two adjacent ATPase sites, which are known to exhibit a sequential pattern of action. In addition, the results presented here provide an atomic level characterization of distinct states in the functional cycle of MutS and MSH2-MSH6. A more open DNA scanning conformation is proposed and a sliding clamp state is predicted whereby the DNA-binding domain is rotated out of the enzyme to result in structures that are significantly different from the crystal structure. These findings should stimulate further experimental and computational studies to validate the predictions made here. In particular, structural experiments could probe the nature of the DNA scanning and sliding conformations based on the predictions presented here, and biochemical studies could test mutations that would disrupt the proposed domain movements. Furthermore, the proposed structures for alternate functional states could be subjected to more extensive computational studies to examine their stability and transitions between those states.

CONCLUSIONS

Results from NM calculations of MSH2-MSH6 and MutS were used to develop a molecular-level picture of distinct conformational states involved in their functional cycles. A comparison of the modes between MSH2-MSH6 and MutS reveals striking similarities, indicating that the two enzymes are not just structurally but also dynamically and functionally equivalent on the molecular level. The most important result indicates the presence of a strong motional correlation between the ATPase domains and the lever domains in all low-frequency modes analyzed, whereas individual modes highlight the specific nature of the correlation between the N-terminal DNA-binding domains and the ATPase domains. This indicates that both MutS and MSH2-MSH6 are structurally capable of establishing long-range allostery during their functional cycle. Based on a detailed analysis of the lowest-frequency modes in the context of the available experimental data, a detailed mechanism is proposed that involves DNA scanning, mismatch recognition, repair initiation, and sliding of MSH2-MSH6/MutS along DNA before scanning is resumed.

NM calculations can provide an approximate view of biologically relevant dynamics in biomolecules, but are limited by the theoretical nature of the methodology. The ideas presented here suggest a number of experiments that could validate and extend the proposed mechanism of DNA mismatch recognition by MSH2-MSH6 and MutS. Furthermore, the NM results can serve as starting points for additional computational studies to investigate the proposed functional states and transitions between them in more detail.

SUPPORTING MATERIAL

Ten movies and five figures are available at http://www.biophysj.org/biophysj/supplemental/S0006-3495(09)00218-5.

We thank Dr. Katarzyna Maksimiak and Mr. Hugh Crosmun for valuable contributions during the early stages of the project, and the High Performance Computing Center at Michigan State University for providing access to computational resources. We acknowledge financial support from the National Science Foundation CAREER Program (grant 0447799) and the Alfred P. Sloan Foundation.

REFERENCES

1. Kunkel, T. A., and D. A. Erie. 2005. DNA mismatch repair. *Annu. Rev. Biochem.* 74:681–710.
2. Modrich, P. 2006. Mechanisms in eukaryotic mismatch repair. *J. Biol. Chem.* 281:30305–30309.
3. Schofield, M. J., and P. Hsieh. 2003. DNA mismatch repair: molecular mechanisms and biological function. *Annu. Rev. Microbiol.* 57:579–608.
4. Peltomaki, P. 2003. Role of DNA mismatch repair defects in the pathogenesis of human cancer. *J. Clin. Oncol.* 21:1174–1179.
5. Obmolova, G., C. Ban, P. Hsieh, and W. Yang. 2000. Crystal structures of mismatch repair protein MutS and its complex with a substrate DNA. *Nature.* 407:703–710.
6. Lamers, M. H., A. Perrakis, J. H. Enzlin, H. H. K. Winterwerp, N. de Wind, et al. 2000. The crystal structure of DNA mismatch repair protein MutS binding to a G-T mismatch. *Nature.* 407:711–717.
7. Grilley, M., K. M. Welsh, S. S. Su, and P. Modrich. 1989. Isolation and characterization of the *Escherichia-coli* Mutl gene product. *J. Biol. Chem.* 264:1000–1004.
8. Gu, L. Y., Y. Hong, S. McCulloch, H. Watanabe, and G. M. Li. 1998. ATP-dependent interaction of human mismatch repair proteins and dual role of PCNA in mismatch repair. *Nucleic Acids Res.* 26:1173–1178.
9. Warren, J. J., T. J. Pohlhaus, A. Changela, R. R. Iyer, P. L. Modrich, et al. 2007. Structure of the human MutS α DNA lesion recognition complex. *Mol. Cell.* 26:579–592.
10. Lamers, M. H., H. H. K. Winterwerp, and T. K. Sixma. 2003. The alternating ATPase domains of MutS control DNA mismatch repair. *EMBO J.* 22:746–756.
11. Antony, E., and M. M. Hingorani. 2004. Asymmetric ATP binding and hydrolysis activity of the *Thermus aquaticus* MutS dimer is key to modulation of its interactions with mismatched DNA. *Biochemistry.* 43:13115–13128.
12. Jacobs-Palmer, E., and M. M. Hingorani. 2007. The effects of nucleotides on MutS-DNA binding kinetics clarify the role of MutS ATPase activity in mismatch repair. *J. Mol. Biol.* 366:1087–1098.
13. Mazur, D. J., M. L. Mendillo, and R. D. Kolodner. 2006. Inhibition of Msh6 ATPase activity by mispaired DNA induces a Msh2(ATP)-Msh6(ATP) state capable of hydrolysis-independent movement along DNA. *Mol. Cell.* 22:39–49.
14. Gorbalenya, A. E., and E. V. Koonin. 1990. Superfamily of Uvra-related Ntp-binding proteins—implications for rational classification of recombination repair systems. *J. Mol. Biol.* 213:583–591.
15. Lamers, M. H., D. Gerogijevic, J. H. Lebbink, H. H. K. Winterwerp, B. Agianian, et al. 2004. ATP increases the affinity between MutS ATPase domains—implications for ATP hydrolysis and conformational changes. *J. Biol. Chem.* 279:43879–43885.
16. Bjornson, K. P., and P. Modrich. 2003. Differential and simultaneous adenosine di- and triphosphate binding by MutS. *J. Biol. Chem.* 278:18557–18562.
17. Lebbink, J. H. G., D. Georgijevic, G. Natrajan, A. Fish, H. H. K. Winterwerp, et al. 2006. Dual role of MutS glutamate 38 in DNA mismatch discrimination and in the authorization of repair. *EMBO J.* 25:409–419.

18. Gorman, J., A. Chowdhury, J. A. Surtees, J. Shimada, D. R. Reichman, et al. 2007. Dynamic basis for one-dimensional DNA scanning by the mismatch repair complex Msh2-Msh6. *Mol. Cell.* 28:359–370.

19. Tama, F., M. Valle, J. Frank, and C. L. Brooks. 2003. Dynamic reorganization of the functionally active ribosome explored by normal mode analysis and cryo-electron microscopy. *Proc. Natl. Acad. Sci. USA.* 100:9319–9323.

20. Van Wynsberghe, A., G. H. Li, and Q. Cui. 2004. Normal-mode analysis suggests protein flexibility modulation throughout RNA polymerase's functional cycle. *Biochemistry.* 43:13083–13096.

21. Fiser, A., R. K. G. Do, and A. Sali. 2000. Modeling of loops in protein structures. *Protein Sci.* 9:1753–1773.

22. Mackerell, A. D., M. Feig, and C. L. Brooks. 2004. Extending the treatment of backbone energetics in protein force fields: limitations of gas-phase quantum mechanics in reproducing protein conformational distributions in molecular dynamics simulations. *J. Comput. Chem.* 25:1400–1415.

23. Li, G. H., and Q. Cui. 2002. A coarse-grained normal mode approach for macromolecules: an efficient implementation and application to Ca^{2+}-ATPase. *Biophys. J.* 83:2457–2474.

24. Tama, F., F. X. Gadea, O. Marques, and Y. H. Sanejouand. 2000. Building-block approach for determining low-frequency normal modes of macromolecules. *Proteins.* 41:1–7.

25. DeLano, W.L. 2002. The PyMOL Molecular Graphics System. DeLano Scientific, Palo Alto, CA.

26. Van Wynsberghe, A. W., and Q. Cui. 2005. Comparison of mode analyses at different resolutions applied to nucleic acid systems. *Biophys. J.* 89:2939–2949.

27. Lu, M., B. Poon, and J. Ma. 2006. A new method for coarse-grained elastic normal-mode analysis. *J. Chem. Theory Comput.* 2:464–471.

28. Kato, R., M. Kataoka, H. Kamikubo, and S. Kuramitsu. 2001. Direct observation of three conformations of MutS protein regulated by adenine nucleotides. *J. Mol. Biol.* 309:227–238.

29. Hays, J. B., P. D. Hoffman, and H. X. Wang. 2005. Discrimination and versatility in mismatch repair. *DNA Repair (Amst.).* 4:1463–1474.

30. Schofield, M. J., F. E. Brownewell, S. Nayak, C. W. Du, E. T. Kool, et al. 2001. The Phe-X-Glu DNA binding motif of MutS—the role of hydrogen bonding in mismatch recognition. *J. Biol. Chem.* 276: 45505–45508.

31. Mitra, R., B. M. Pettitt, G. L. Rame, and R. D. Blake. 1993. The relationship between mutation-rates for the (C-G)→(T-A) transition and features of T-G mispair structures in different neighbor environments, determined by free-energy molecular mechanics. *Nucleic Acids Res.* 21:6028–6037.

32. Hiratsuka, T. 1994. Nucleotide-induced closure of the ATP-binding pocket in myosin subfragment-1. *J. Biol. Chem.* 269:27251–27257.

33. Bilwes, A. M., C. M. Quezada, L. R. Croal, B. R. Crane, and M. I. Simon. 2001. Nucleotide binding by the histidine kinase CheA. *Nat. Struct. Biol.* 8:353–360.

34. Janas, E., M. Hofacker, M. Chen, S. Gompf, C. van der Does, et al. 2003. The ATP hydrolysis cycle of the nucleotide-binding domain of the mitochondrial ATP-binding cassette transporter Mdl1p. *J. Biol. Chem.* 278:26862–26869.

35. Gradia, S., D. Subramanian, T. Wilson, S. Acharya, A. Makhov, et al. 1999. hMSH2-hMSH6 forms a hydrolysis-independent sliding clamp on mismatched DNA. *Mol. Cell.* 3:255–261.

36. Pluciennik, A., and P. Modrich. 2007. Protein roadblocks and helix discontinuities are barriers to the initiation of mismatch repair. *Proc. Natl. Acad. Sci. USA.* 104:12709–12713.